Communication

Efficient Shaped Pattern Synthesis for Time Modulated Antenna Arrays Including Mutual Coupling by Differential Evolution Integrated with FFT via Least-Square Active Element Pattern Expansion

Yanhui Liu, *Senior Member, IEEE*, Jingjing Bai, Jinxiang Zheng, Haiyan Liao, Yi Ren, and Y. Jay Guo, *Fellow, IEEE*

***Abstract*—The fast Fourier transform (FFT) via the least-square active element pattern expansion (LSAEPE) is generalized to speed up the computation of array patterns including mutual coupling and platform effect for time-modulated antenna arrays (TMAAs) at the central and sideband frequencies. By integrating the LSAEPE-FFT with differential evolution algorithm (DEA), the resulting DEA-LSAEPE-FFT method can realize efficient shaped pattern synthesis with accurate control of mainlobe shape, sidelobe level (SLL) and sideband level (SBL). Two examples of synthesizing different shaped patterns for different TMAAs mounted on a nonuniform platform or with metal scatters are conducted to validate the effectiveness and robustness of the proposed method. Synthesis results show that the proposed method has much better accuracy performance than the conventional DEA-FFT while costing much less CPU time than that of using DEA combined with direct summation.**

***Index Terms*—Time modulated antenna array (TMAA), least-square active element pattern expansion (LSAEPE), fast Fourier transform (FFT), differential evolution algorithm (DEA), mutual coupling.**

I. Introduction

SHAPED beam antenna arrays have been widely used in many applications such as satellite communication, sensing and radar systems. In the past several decades, many advanced shaped pattern synthesis methods have been presented, such as the analytical techniques [1], [2], alternating projection methods [3], mathematical optimization techniques [4], [5], and stochastic optimization algorithms [6], [7]. However, in order to achieve the desired shaped radiation patterns, most of these methods aim at optimizing both the static excitation amplitudes and phases. This requires a relatively complicated radio-frequency (RF) feeding network for implementing simultaneous amplitude and phase weighting. In particular, multiple unequal power dividers need be carefully designed.

It is known that using time modulation through controlling the high-speed RF switches can realize an equivalent amplitude weighting for antenna arrays [8]. This idea has been widely applied to obtain low-sidelobe focused beam patterns [9]–[14] as well as shaped power patterns [15]–[18], by using either uniform static excitation amplitudes or a relatively low dynamic range ratio (DRR) of static amplitudes. By periodically controlling the 'switch-on' time durations of the RF switches, various equivalent amplitude distributions can be generated, and in particular some complicated asymmetrical excitation distributions can be easily obtained. Thus time-modulated antenna arrays (TMAAs) are suitable for producing shaped patterns with electrically adjustable pattern shapes and sidelobe distributions. However, most of shaped pattern synthesis techniques for time-modulated antenna arrays deal with only the array factor, and the mutual coupling and platform effect for a practical TMAA is usually ignored in the pattern synthesis. This causes the synthesized TMAA pattern deviating from the real one where mutual coupling cannot be simply ignored for most antenna array structures. To solve the problem, one can introduce simulated or measured active element patterns into the TMAA pattern synthesis so that the mutual coupling is included [19]. In [20], an iterative convex optimization method is presented in which mutual coupling and port matching have been effectively incorporated into the TMAA synthesis by considering the AEP and active reflection coefficient (ARC). A detailed analysis of mutual coupling effect on the TMAA pattern in both time and frequency-domain can be found in [21].

For a typical TMAA using single-pole single-throw (STST) switches, synthesizing a shaped pattern usually requires to optimize the time modulation parameters such as 'switch-on' time durations, starting instants and possible excitation phases for the elements. This is usually done by calling some stochastic optimization algorithms such as the differential evolution algorithm (DEA) [22]–[25]. In these algorithms, a large number of repeated computations of array patterns at central frequency and sidebands are required which cost the most part of the whole time cost for this optimization problem. As is known, the Fourier transform (FT) relationship exists between the excitation distribution and array factor of a uniformly spaced array. This relationship has been widely utilized in efficient pattern synthesis for conventional frequency-domain arrays [26]–[28]. In the TMAA application, relatively less discussion has been given to the problem of efficient array pattern computation. Nevertheless, few techniques in [29]–[31] have been presented to apply the FT relationship to speed up the TMAA pattern computation. However, these efficient techniques process only the array factor without considering mutual coupling since the regular FFT used cannot deal with the variation of element patterns among different elements of a practical TMAA. To the best of our knowledge, how to apply the FFT to efficiently synthesize a shaped pattern with accurate control of mainlobe shape, sidelobe distribution and sideband level for the TMAA including mutual coupling remains a very challenging problem.

In this work, we introduce a least-square active element pattern expansion (LSAEPE) method to deal with the pattern synthesis of linear TMAAs including mutual coupling and platform effect. The LSAEPE was integrated into the iterative FFT procedure for efficient pattern synthesis of conventional frequency-domain antenna arrays including mutual coupling [32], [33]. In this method, active element patterns (AEPs) are adopted to include mutual coupling in the array pattern [34], and each AEP is approximated as the radiation from several nearby virtual elements that are free of mutual coupling so that the AEP can be approximated by a weighted summation

Manuscript received xxx. This work was supported by the Natural Science Foundation of China (NSFC) under Grant No. 61871338 and 61871063. (Corresponding author: Yanhui Liu and Yi Ren)

Y. Liu is with the School of Electronic Science and Engineering and also the Yangtze Delta Region Institute (Quzhou), University of Electronic Science and Technology of China, China. (email: yhliu@uestc.edu.cn).

J. Bai, J. Zheng, and H. Liao are with the Institute of Electromagnetics and Acoustics, Xiamen University, Fujian 361005, China. J. Bai is also with the Yangtze Delta Region Institute (Quzhou), University of Electronic Science and Technology of China, Zhejiang 324000, China.

Y. Ren is with School of Electronic Engineering, Xidian University, Xi'an 710071, China.(email: renyi_cq@hotmail.com)

Y. Jay Guo is with the Global Big Data Technologies Centre, University of Technology Sydney (UTS), NSW 2007, Australia.

of several phase-shifted element patterns. The optimal weighting coefficients can be obtained by minimizing the LS approximation error. In this work, the FFT via LSAEPE is further generalized to deal with the efficient pattern computation for linear TMAAs. The approximated array pattern expressions by using the LSAEPE at both central and sideband frequencies are derived so that the FFT can be applied to speed up the computation of array pattern including mutual coupling of a TMAA at all harmonic frequencies. This LSAEPE-FFT is integrated into the DEA optimization so that appropriate 'switch-on' time durations, starting instants and static excitation phases can be efficiently found for producing a desired pattern with accurate control of mainlobe shape, sidelobe level (SLL) and sideband level (SBL). Two examples of synthesizing cosecant-squared and flat-top patterns for different linear TMAAs mounted on different platforms are conducted to validate the effectiveness and advantages of the proposed technique.

II. Methodology and Algorithms

A. Time-modulated antenna array with mutual coupling

Consider a time-modulated antenna array (TMAA) consisting of N antenna elements with spacing of d aligned at x-axis. As shown in Fig. 1, each element in the array is connected to a phase shifter followed by a high speed RF switch. Here assume that uniform static excitation amplitude is used for each element. The array pattern including mutual coupling can be written as

$$F(u,t) = e^{j2\pi f_0 t} \sum_{n=0}^{N-1} U_n(t) e^{j\phi_n} g_n(u) e^{j\beta n d u} \tag{1}$$

where $u = \sin\theta$, $\beta = 2\pi f_0/c$ is the wavenumber at the central frequency f_0, ϕ_n is the excitation phase for the nth element, $U_n(t)$ is the periodic time-modulation function used to model the status of the RF switch for nth element, and $g_n(u)$ is the active element pattern (AEP) of the nth element which can be used to include mutual coupling and platform effect on the array pattern performance [34].

Assume that the time modulation function is modeled as a periodic pulse function that can be given by [11]

$$U_n(t) = \begin{cases} 1, & t_n^{\text{on}} \le t \le t_n^{\text{on}} + t_n^{\text{pin}} \\ 0, & \text{otherwise} \end{cases} \tag{2}$$

where t_n^{on} is the switch-on instant of the n-th element, and t_n^{pin} is the 'switch-on' duration time over one period of T_P. In general, we have $0 \le t_n^{\text{on}} \le T_P$ and $0 \le t_n^{\text{pin}} \le T_P$. Such a time modulation is called the pulse shifting (PS) mode for the TMAA [11]. When all t_n^{on}s are equal to zeros, it reduce to the variable aperture size (VAS) mode [25]. By expanding the periodic function $U_n(t)$ as the sum of Fourier series, we obtain the array patterns at the central frequency f_0 and mth sideband frequency $f_m = f_0 + mf_P$ ($m = 0, \pm1, \pm2, \cdots, \pm\infty$)

$$F_m(u) = \sum_{n=0}^{N-1} \frac{\sin(m\pi\tau_n^{\text{pin}})}{m\pi} e^{-jm\pi(\tau_n^{\text{pin}} + \frac{2t_n^{\text{on}}}{T_p})} e^{j\phi_n} g_n(u) e^{j\beta n d u} \tag{3}$$

where $\tau_n^{\text{pin}} = t_n^{\text{pin}}/T_P$ is the normalized 'switch-on' duration time, and $f_P = 1/T_P$ is the time modulation frequency. Usually, we have $T_p \ll 1/f_0$ and thus $f_P \ll f_0$. In this situation, the AEP $g_n(u)$ remains almost unchanged over the sideband frequencies nearby the central frequency (e.g., $|m| \le 2$).

B. Efficient Computation of TMAA Array Patterns Including Mutual Coupling using FFT via LSAEPE

Due to the mutual coupling effect in the antenna array environment, the AEPs vary among different elements. Consequently, the array pattern expression in (3) cannot be efficiently computed by using the regular FFT and it is usually obtained by direct summation [11]. Here, we introduce a least-square active element pattern expansion (LSAEPE) method which was presented in [32] to deal with the efficient computation of the array pattern including mutual coupling for conventional antenna arrays without time-modulation. The basic idea of the LSAEPE is approximating the AEP of an antenna element as a radiation pattern from a virtual subarray consisting of several nearby elements round this element. This virtual subarray is assumed to be free of mutual coupling, and thus each element has the same element pattern that is approximately obtained by averaging all the original AEPs. That is, finding the following approximation for $n = 0, 1, \cdots, N-1$

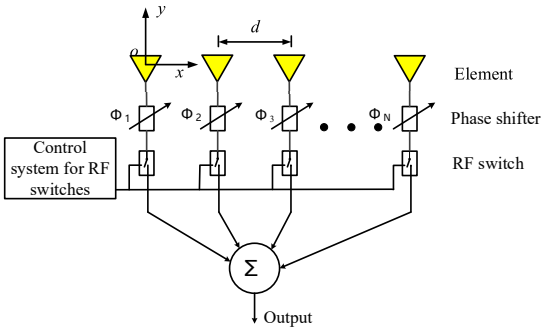

Fig. 1. Schematic diagram of a TMAA with RF switches and phase shifters.

$$g_n(u) \approx g_{\text{ave}}(u) \sum_{q=-Q/2}^{Q/2} c_{n,q} e^{j\beta q d u} \tag{4}$$

where Q is the number of elements used to approximate the AEP, and $g_{\text{ave}}(u) = \sum_{n=0}^{N-1} g_n(u)/N$ represents the averaged element pattern. To deal with the edge elements, $Q/2$ virtual elements should be added into each side of the concerned array. Thus, the virtual enlarged array has a total of $(N+Q)$ elements. The coefficient c_{nq} denotes the coupling contribution from the $(n+q)$th element to the nth element, and it can be obtained by solving the following LS minimization problem

$$\min_{c_n} \|\mathbf{g}_n - \mathbf{Z}\mathbf{c}_n\|_2^2 \tag{5}$$

where

$$\mathbf{c}_n = \left[c_{n,-\frac{Q}{2}}, c_{n,-\frac{Q}{2}+1}, \cdots, c_{n,\frac{Q}{2}}\right]^T \tag{6}$$

$$\mathbf{g}_n = [g_n(u_1), g_n(u_2), \cdots, g_n(u_M)]^T \tag{7}$$

$$\mathbf{Z} = \begin{pmatrix} g_{\text{ave}}(u_1)e^{j\beta d u_1(-\frac{Q}{2})} & \cdots & g_{\text{ave}}(u_1)e^{j\beta d u_1(\frac{Q}{2})} \\ \vdots & \ddots & \vdots \\ g_{\text{ave}}(u_M)e^{j\beta d u_M(-\frac{Q}{2})} & \cdots & g_{\text{ave}}(u_M)e^{j\beta d u_M(\frac{Q}{2})} \end{pmatrix} \tag{8}$$

The solution to the above problem is given by $\mathbf{c}_n = (\mathbf{Z}^H\mathbf{Z})^{-1}\mathbf{Z}^H\mathbf{g}_n$.

By incorporating the approximate expansion of (4) into (3), the array pattern at mth harmonic frequency can be rewritten as:

$$F_m(u) = g_{\text{ave}}(u)\, e^{-j\beta d u \frac{Q}{2}} \sum_{l=0}^{L-1} a_l^{(m)} e^{j\beta l d u} \tag{9}$$

where $L = N + Q$, and

$$a_l^{(m)} = \sum_{\substack{l=n+q+Q/2 \\ -Q/2 \le q \le Q/2}} c_{n,q} w_n^{(m)} \tag{10}$$

$$w_n^{(m)} = \begin{cases} \tau_n^{\text{pin}} e^{j\phi_n}, & m = 0 \\ \frac{\sin(m\pi\tau_n^{\text{pin}})}{m\pi} e^{j\phi_n - jm\pi(\tau_n^{\text{pin}} + \frac{2t_n^{\text{on}}}{T_p})}, & m \ne 0 \end{cases} \tag{11}$$

It is observed that with the help of the LSAEPE, the array pattern at either the central frequency or each harmonic frequency f_m ($m =$

$0, \pm 1, \cdots, \pm\infty$) can be approximated as the discrete spatial Fourier transform of the excitation distribution $\{a_l^{(m)}\}$ for the virtual enlarged array. By uniformly sampling the variable u with $u_k = k\Delta_u$ where $\Delta_u = 2\pi/(K\beta d)$ and $k = -K/2, \cdots, K/2$ ($K \geq L$), we have

$$F_m(k\Delta_u) = g_{\text{ave}}(k\Delta_u)e^{-j\pi Qk/K}\sum_{l=0}^{L-1} a_l^{(m)} e^{j2\pi lk/K} \tag{12}$$

Clearly, the above summation can be efficiently computed by using the regular FFT. If the radix-2 FFT is used, computing K-point pattern results at each f_m will require about $K/2\log_2 K+(Q+1)L+K+N$ complex multiplications while it requires about $NK+N$ complex multiplications for the case of using direct summation.

C. Shaped Pattern Optimization for TMAA Using DEA-FFT-LSAEPE

The problem concerned is obtaining a desired shaped mainlobe at a central frequency while suppressing the sidelobe level (SLL) and sideband level (SBL) by optimizing the normalized 'switch-on' time τ_n^{pin}, starting instant t_n^{on} and static excitation phase ϕ_n for $n = 0, 1, \cdots, N-1$ in the TMAA. By setting the optimization vector $\boldsymbol{v} = \{(\tau_0^{\text{pin}}, t_0^{\text{on}}, \phi_0), \cdots, (\tau_{N-1}^{\text{pin}}, t_{N-1}^{\text{on}}, \phi_{N-1})\}$, this problem can be formulated as minimizing the following fitness function

$$\begin{aligned} f(\boldsymbol{v}) =& \frac{W_1}{N_S}\sum_{u_s\in U_S}\left||F_0(u_s;\boldsymbol{v})|^2 - P_d(u_s)\right| \\ &+ W_2|SLL_{\max}(\boldsymbol{v}) - SLL_d|^2 H(SLL_{\max}(\boldsymbol{v}) - SLL_d) \\ &+ W_3|SBL_{\max}(\boldsymbol{v}) - SBL_d|^2 H(SBL_{\max}(\boldsymbol{v}) - SBL_d) \\ &+ W_4|\eta_{\text{sw}}(\boldsymbol{v}) - \eta_d|^2 H(\eta_{\text{sw}}(\boldsymbol{v}) - \eta_d) \end{aligned} \tag{13}$$

where the parameters $W1$, $W2$, $W3$ and $W4$ are weighting factors which are used to penalize the terms with appropriate weights in the cost function. $u_s \in U_S$ denotes the shaped mainlobe region in u-space, N_S is the number of pattern sampling points in this region , $P_d(u_s)$ denotes the desired mainlobe power distribution, and $H(\cdot)$ denotes a heaviside function. $SLL_{\max}(\boldsymbol{v}) = \max_{u\notin U_S}|F_0(u;\boldsymbol{v})|^2$ denotes the maximum SLL at the central frequency, and $SBL_{\max}(\boldsymbol{v}) = \max\{\max_u|F_{\pm1}(u;\boldsymbol{v})|^2, \cdots, \max_u|F_{\pm M}(u;\boldsymbol{v})|^2\}$ denotes the maximum SBL among M harmonic components. For typical VAS and PS modes, we consider only the first harmonic component (i.e., $M = 1$) since the SBL is decaying with the index of harmonic frequency. η_{sw} is the switch efficiency defined by $\eta_{\text{sw}} = \sum_{n=1}^{N}\tau_n^{\text{pin}}/N$ in [35].

The optimization of the 'switch-on' time τ_n^{pin}, starting instant t_n^{on} and static excitation phase ϕ_n is a highly non-linear problem. Thus, generally some stochastic optimization algorithms will be adequate. Here we choose to utilize the differential evolution algorithm (DEA) since it is a simple but powerful stochastic global optimizer. The DEA has been proved to be a very effective algorithm for solving many antenna array synthesis problems including the TMAA optimization [22]–[25]. Like the genetic algorithm, the DEA is also a population-based algorithm which finds the optimal solution through a number of population updating. In the DEA-based optimization, N_p individuals consisting of different $\boldsymbol{v} = \{(\tau_0^{\text{pin}}, t_0^{\text{on}}, \phi_0), \cdots, (\tau_{N-1}^{\text{pin}}, t_{N-1}^{\text{on}}, \phi_{N-1})\}$ will be randomly generated in the beginning, and their fitness values will be evaluated by using the fitness function (13). Then, in each generation, the optimal individual will be mutated to produce trail vectors which are then used to carry out the crossover operation with other non-optimal individuals to generate new individuals. The new generated individuals will compete with the non-optimal who generate them in the crossover for a position to the next generation. The evolution will continue unless the optimal individual remain unchanged for many times or the allowed maximum generation M_g is reached. Clearly, a huge number of repeated calculations of (13) are required in the DEA to evaluate the performance of every individual of the population in iteration. Fortunately, we can adopt the FFT via LSAEPE to speed up the computation of the array patterns at the central frequency and sideband as shown in (12). Note that in the LSAEPE method, for different individuals with varying $(\tau_n^{\text{pin}}, \phi_n)$ for $n = 0, \cdots, N-1$, all the coupling coefficients $c_{n,q}$ need to be computed only once for a given antenna array geometry. The resulting synthesis procedure is called the DEA-LSAEPE-FFT method which can save much CPU time compared with the way of using the DEA combined with direct summation in (3). Note that this method can be directly applied to the pattern synthesis for the TMAA with VAS mode by simply presetting all t_n^{on}s to be zeros.

III. Numerical Results

In this section, two examples for synthesizing a cosecant-squared pattern for a TMAA with microstrip antenna elements and a flat-top pattern for a TMAA with many nearby scatters are provided to validate the effectiveness and robustness of the proposed strategy. The comparison with other methods is also given in the examples. All the synthesis examples except for the part of full-wave simulation were run in the same personal computer with Intel Core i3-4160@3.6GHz and 4 GB RAM.

A. Cosecant-squared pattern synthesis for a TMAA with 48 microstrip antenna elements backed on a trapezoidal metal ground

In the first example, we consider synthesizing a cosecant-squared pattern for a 48-element TMAA backed on a trapezoidal metal ground with VAS mode. The geometry of this array is shown in Fig. 2. The microstrip antennas elements work at the central frequency of 2.45 GHz, and the element spacing is 48.95 mm that is about 0.4λ at 2.45 GHz. Assume that the desired pattern has a cosecant-squared mainlobe shape at the central frequency and the pattern levels at the sidelobe region and the first sideband is less than a -22 dB bound (i.e., $SLL_d = SBL_d = -22$ dB), as shown in Fig. 3. Now, we consider to apply the time modulation technique to produce such a shaped pattern. Assume that the VAS mode with a time modulation frequency of $f_P = 1$ MHz is adopted in this example. First, we apply the DEA-FFT method to optimize the normalized 'switch-on' time τ_n^{pin} and static excitation phase ϕ_n for $n = 0, 1, \cdots, N-1$. In this method, the array pattern is synthesized without considering mutual coupling and element characteristics. For the DEA optimization, the number of individuals in the population is set as $N_p = 288$ that is three times of the number of optimization variables, and the allowable maximum umber of iterations is set as $M_g = 3000$. The number of pattern sampling points is set as $K = 1024$, and the weighting factors in the fitness function are chosen as $W_1 = 0.5$ and $W_2 = W_3 = W_4 = 1$. The obtained array patterns at the central frequency and the first sideband are shown in Fig. 3(a). As can be seen, the synthesized mainlobe at the central frequency approximates the desired cosecant-squared shape very well, and the SLL as well as the SBL also reach their boundary requirements. However, when considering the real antenna array structure, the real array patterns at the central and sideband frequencies by using full-wave simulated AEPs with the equivalent excitations calculated by the same 'switch-on' durations and excitation phases at the corresponding frequencies deviates much from the synthesized ones. As shown in Fig. 3(a), the synthesized real pattern mainlobe is considerably higher than the desired shape in the region of $\theta \in [-25^\circ, -5^\circ]$ and the maximum mainlobe deviation from the desired one is 0.71 dB. The SLL and SBL for the real patterns are -18.32 dB and -19.91 dB, respectively. The real SLL is 3.68 dB higher than the desired upper bound.

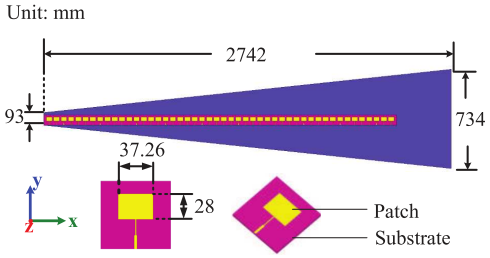

Fig. 2. The geometry of a TMAA with 48 microstrip patch antenna elements backed on a trapezoidal metal ground.

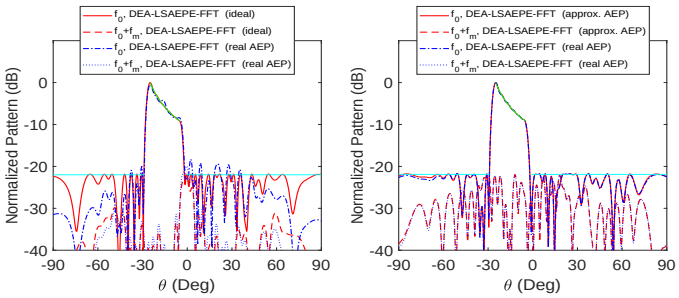

Fig. 3. The synthesized patterns as well as the corresponding real array patterns including mutual coupling and platform effect obtained by using simulated AEPs with the equivalent excitations calculated by the same 'switch-on' durations and excitation phases. The results are obtained by (a) the DEA-FFT and (b) the proposed DEA-LSAEPE-FFT, respectively.

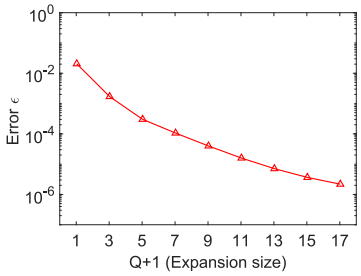

Fig. 4. Approximation error ϵ versus different $(Q+1)$ in Example 1.

Now, we apply the proposed DEA-LSAEPE-FFT method to synthesize the same desired pattern for this TMAA. All the simulated AEPs are used, and each AEP is approximated by $(Q+1)$ virtual elements. The expansion approximation error can be given by

$$\epsilon = \frac{\sum_{n=0}^{N-1} \|\boldsymbol{g}_n - \boldsymbol{Z}\boldsymbol{c}_n\|_2^2}{\sum_{n=0}^{N-1} \|\boldsymbol{g}_n\|_2^2} \tag{14}$$

Fig. 4 shows the error ϵ versus different $(Q+1)$ for this TMAA. As can be seen, as the expansion size of $(Q+1)$ increases, the approximation error ϵ decreases stably. In this example, we choose $Q=2$ for $\epsilon \leq 1\%$ to achieve a good balance between efficiency and accuracy performances. The parameters setting for the DEA is the same as that of the DEA-FFT. The obtained synthesized and real array patterns (with approximated and real AEPs, respectively) at central frequency and first sideband are given in Fig. 3(b). As can be seen, the synthesized array patterns agree well with the real ones at both central frequency and sideband. The maximum mainlobe deviation from the desired shape is only 0.15 dB that is much smaller than the 0.71 dB deviation by the DEA-FFT. The SLL and SBL are -21.61 dB and -21.88 dB, respectively, and they are much lower than the corresponding results by the DEA-FFT. The maximum gains of the cosecant-squared mainlobe are 11.72 dB and 12.03 dB for the DEA-FFT and the proposed DEA-LSAEPE-FFT method, respectively.

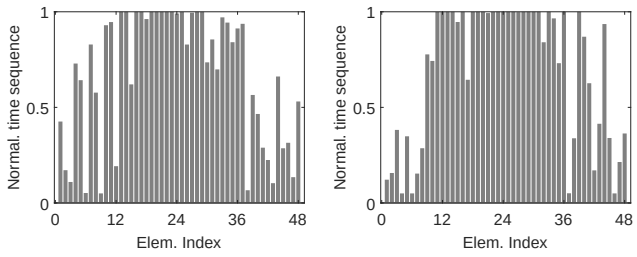

Fig. 5. The synthesized normalized switch-on time durations for the cosecant-squared pattern of the 48-element TMAA with VAS mode by (a) the DEA-FFT and (b) the DEA-LSAEPE-FFT.

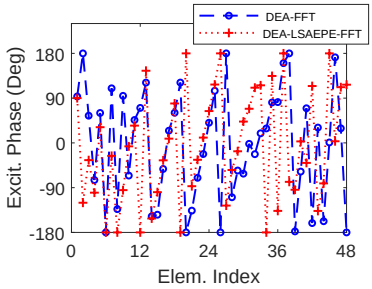

Fig. 6. The synthesized static excitation phases for the cosecant-squared pattern by the DEA-FFT and the proposed DEA-LSAEPE-FFT.

Fig. 5 and 6 show the normalized 'switch-on' duration times and static excitation phases obtained by the DEA-FFT and the proposed DEA-LSAEPE-FFT, respectively. Due to the inclusion of the mutual coupling and platform effect, the synthesized results by the proposed method considerably vary from those by the DEA-FFT. In this example, the DEA-FFT takes 1.78 minutes, and the proposed method takes about 1.98 minutes. It should be noted that if the direct summation in (3) is used to include the mutual coupling and platform effect, the whole DEA-based optimization costs 9.83 minutes to obtain synthesis results that are comparable to those by the proposed DEA-LSAEPE-FFT. The summary of the synthesis results obtained by the three methods are provided in Table I. We can see that the proposed method has much better accuracy performance than the conventional DEA-FFT while costs much less CPU time than the method using the DEA combined with direct summation.

B. Flat-top pattern of a TMAA with bowtie antenna elements surrounded by some nearby scatters

In the second example, we consider synthesizing a shaped pattern for a TMAA in a more complicated environment. As shown in Fig. 7, the TMAA has 20 printed bowtie antenna elements working at the central frequency of 9.82 GHz. The element spacing is 15.25 mm that is about 0.5λ at 9.82 GHz. This array is surrounded with some metal scatters that model mechanical parts such as fixtures or supporting structures in a practical environment. In this example, assume that the PS mode with a time modulation frequency of $f_P = 1$ MHz is adopted. The desired pattern at the central frequency is assumed to have a flat-top mainlobe in the region $\theta \in [-15°, 15°]$, and the desired SLL is set as -22 dB in the region of $|\theta| \geq 21.5°$. The SBL bound is also set as -22 dB. For comparison, we also apply the conventional DEA-FFT, the DEA combined with direct summation and the proposed DEA-LSAEPE-FFT to synthesize this example. The number of optimization variables is 60 by using the PS time modulation. We set $Np = 180$ for the population size, and other parameters including the maximum iterations, the number

TABLE I
THE PERFORMANCE SUMMARY OF SYNTHESIZING COSECANT-SQUARED AND FLAT-TOP PATTERNS BY THE THREE METHODS

Synthesis Method	Cosecant-squared pattern case ($N = 48$, VAS time modulation)							
	The synthesized array pattern			The real pattern using AEPs			η_{sw}	Time (min)
	Ripple (dB)	SLL_{max} (dB)	SBL_{max} (dB)	Ripple (dB)	SLL_{max} (dB)	SBL_{max} (dB)		
DEA-FFT	± 0.11	-21.83	-21.94	± 0.71	-18.32	-19.91	67.2%	1.78
DEA-LSAEPE-FFT	± 0.12	-21.86	-21.92	± 0.15	-21.61	-21.88	69.3%	1.98
DEA+direct sum	– –	– –	– –	± 0.20	-21.72	-21.81	67.8%	9.83
	Flat-top patten case ($N = 20$, PS time modulation)							
DEA-FFT	± 0.41	-21.98	-22.05	± 1.82	-17.82	-20.76	55.7%	1.33
DEA-LSAEPE-FFT	± 0.26	-21.96	-22.10	± 0.40	-21.07	-22.16	54.6%	1.47
DEA+direct sum	– –	– –	– –	± 0.32	-21.58	-22.02	53.9%	4.95

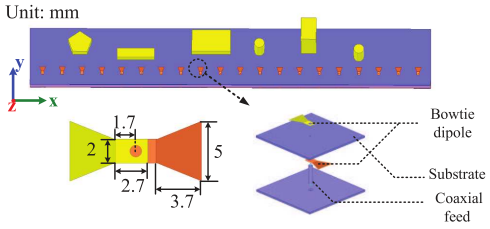

Fig. 7. The geometry of a TMAA with 20 bowtie antenna elements surrounded with some metal scatters.

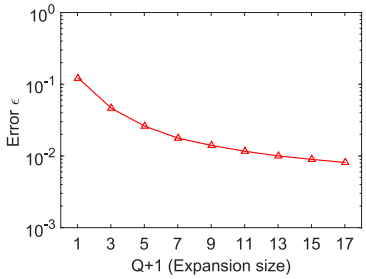

Fig. 8. Approximation error ϵ versus different $(Q+1)$ in Example 2.

of pattern sampling points and the weighting factors are used as the same as those in Example 1. In this example, the approximation error ϵ versus different $(Q+1)$ is shown in Fig. 8. Due to the presence of nearby scatterers, the approximation error is considerably higher than that of the first example. In this case, $Q = 12$ is required for the approximation error $\epsilon \leq 1\%$.

Fig. 9(a) and (b) show the synthesized and real array patterns obtained by the DEA-FFT and the proposed method, respectively. It can be seen that although the synthesized array patterns at both central frequency and sideband by the DEA-FFT are satisfactory, the performance of the corresponding real array patterns deteriorates significantly due to the mutual coupling and scattering effect. The SBL is increased from -22.05 dB to -20.76 dB and the SLL is increased from -21.98 dB to -17.82 dB. This is not the case for the proposed method. Due to the usage of the AEPs by the LSAEPE-FFT, the synthesized and real array patterns by the proposed method match very well with each other at both the central frequency and sideband, as shown in Fig. 9(b). The SLL and SBL for the real patterns are -21.07 dB and -22.16 dB, respectively. The averaged gain over the mainlobe region is 11.86 dB and 11.73 dB obtained by the DEA-FFT and the proposed method, respectively. Fig. 10 and Fig. 11 show the normalized 'switch-on' time sequences and static excitation phases obtained by the DEA-FFT and the proposed DEA-LSAEPE-FFT, respectively.

The results obtained by the DEA combined direct summation are similar as those by the proposed method. The pattern performances by all the three methods for this array are also summarized in Table I. The time costs are 1.33, 1.47 and 4.95 minutes for the DEA-FFT, the proposed method and the DEA plus direct summation. Again, the proposed method costs much less CPU time while obtaining as good pattern performance as that of the DEA combined with direct summation.

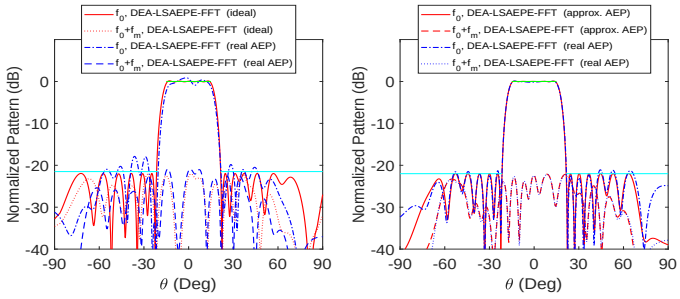

(a) (b)

Fig. 9. The synthesized flat-top patterns as well as the corresponding real array patterns for the 20-element TMAA with PS mode including mutual coupling and platform effect. The results are obtained by (a) the DEA-FFT and (b) the proposed DEA-LSAEPE-FFT, respectively.

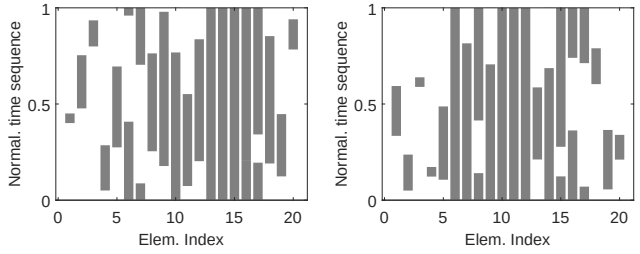

(a) (b)

Fig. 10. The synthesized normalized switch-on time durations for the cosecant-squared pattern by (a) the DEA-FFT and (b) the DEA-LSAEPE-FFT.

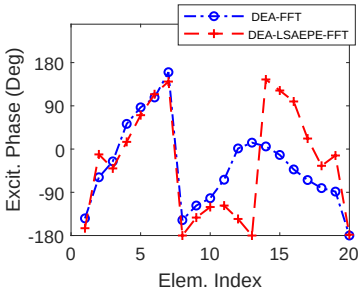

Fig. 11. The synthesized static excitation phases for the flat-top pattern by the DEA-FFT and the proposed DEA-LSAEPE-FFT.

IV. Conclusion

In this paper, a novel shaped pattern synthesis method called the DEA-LSAEPE-FFT has been proposed to synthesize shaped patterns by optimizing the 'switch-on' time durations, starting instants and static excitation phases of TMAAs. By generalization of the LSAEPE-FFT, the array patterns of a TMAA including mutual coupling and platform effect at central frequency and sideband can be efficiently computed. Two examples for synthesizing a cosecant-squared pattern for a 64-element TMAA with VAS mode on a trapezoidal metal ground and a flat-top pattern for a 32-element TMAA with PS mode surrounded with some metal scatterers are provided. Synthesis results show that the proposed method can obtain much more accurate synthesis results with better control of mainlobe shape, SLL and SBL than the conventional DEA-FFT while costing much less CPU time than the DEA conbined with direct summation. On the other hand, it is also mentioned that the current technique is based on the typical TMAA structure using SPST switches, and static phase shifters are required to radiate a shaped pattern at the central frequency. These static phase shifters can be probably avoided if adopting a non-uniform period modulation presented in [14] where reconfiguring among several delay lines is used in each channel.

Finally, it should be noted that the proposed idea can be further generalized to efficiently synthesize the pattern of a planar TMAA. However, in that situation, one would deal with a vectorial array pattern probem by considering both $\vec{e}_\theta$- and $\vec{e}_\phi$-polarized components. In addition, all the AEPs obtained in (θ, ϕ)-space should be interpolated onto the (u, v)-space such that the FFT via LSAEPE can be performed to speed up the pattern computation for planar TMAAs. Such an extension is very interesting and worthy of further study.

References

[1] P. M. Woodward and J. D. Lawson, "The theoretical precision with which an arbitrary radiation pattern may be obtained from a source of a finite size," *J. IEE*, vol. 95, no. 37, pt. III, pp. 363-370, Sep. 1948.

[2] J.-Y. Li, Y.-X. Qi, and S.-G. Zhou, "Shaped beam synthesis based on superposition principle and Taylor method," *IEEE Trans. Antennas Propag.*, vol. 65, no. 11, pp. 6157-6160, Sep. 2017.

[3] J. L. A. Quijano and G. Vecchi, "Alternating adaptive projections in antenna synthesis," *IEEE Trans. Antennas Propag.*, vol. 58, no. 3, pp. 727-737, Mar. 2010.

[4] B. Fuchs, "Application of convex relaxation to array synthesis problems," *IEEE Trans. Antennas Propag.*, vol. 62, no. 2, pp. 634-640, Feb. 2014.

[5] Y. Liu, J. Bai, K. D. Xu, Z. Xu, F. Han, Q. H. Liu, and Y. Jay Guo, "Linearly polarized shaped power pattern synthesis with sidelobe and cross-polarization control by using semidefinite relaxation," *IEEE Trans. Antennas Propag.*, vol. 66, no. 6, pp. 3207-3212, Jun. 2018.

[6] F. J. Ares-Pena, J. A. Gonzalez, E. Lopez, and S. R. Rengarajan, "Genetic algorithms in the design and optimization of antenna array patterns," *IEEE Trans. Antennas Propag.*, vol. 47, no. 3, pp. 506-510, Mar. 1999.

[7] A. Pirhadi, M. H. Rahmani, and A. Mallahzadeh, "Shaped beam array synthesis using particle swarm optimisation method with mutual coupling compensation and wideband feeding network," *IET Microw., Antennas Propag.*, vol. 8, no. 8, pp. 549-555, Jun. 2014.

[8] H. E. Shanks and R. W. Bickmore, "Four-dimensional electromagnetic radiators," *Canadian Journal of Physics*., vol. 37, no. 3, pp. 263-275, Jan. 1995.

[9] S. Yang, Y. B. Gan, and A. Qing, "Sideband suppression in time-modulated linear arrays by the differential evolution algorithm," *IEEE Antennas Wireless Propag. Lett.*, vol. 1, pp. 173-175, 2002.

[10] J. Fondevila, J. C. Bregains, F. Ares, and E. Moreno, "Optimizing uniformly excited linear arrays through time modulation," *IEEE Antennas Wireless Propag. Lett.*, vol. 3, no 1, 298-301, 2004.

[11] L. Poli, P. Rocca, L. Manica and A. Massa, "Pattern synthesis in time-modulated linear arrays through pulse shifting," *IET Microwaves, Antennas Propag.*, vol. 4, no. 9, pp. 1157-1164, Sep. 2010.

[12] C. He, H. Yu, X. Liang, J. Geng, and R. Jin, "Sideband radiation level suppression in time-modulated array by nonuniform period modulation," *IEEE Antennas Wireless Propag. Lett.*, vol. 14, pp. 606-609, 2015.

[13] Z. J. Jiang , S. Zhao, Y. Chen, and T. J. Cui, "Beamforming optimization for time-modulated circular-aperture grid array with DE algorithm", *IEEE Antennas Wireless Propag. Lett.*, vol. 17, no. 12, pp. 2434 - 2438, 2018.

[14] G. Ni, C. He, J. Chen, Y. Liu, and R. Jin, "Low sideband radiation beam scanning at carrier frequency for time-modulated array by non-uniform period modulation," *IEEE Trans. Antennas Propag.*, vol. 68, no. 5, pp. 3695-3704, May 2020.

[15] S. Yang, Y. B. Gan, and P. K. Tan, "A new technique for power-pattern synthesis in time-modulated linear arrays," *IEEE Antennas Wireless Propag. Lett.*, vol. 2, no. 1, pp. 285-287, 2003.

[16] L. Poli, P. Rocca, G. Oliveri, and A. Massa, "Harmonic beamforming in time-modulated linear arrays," *IEEE Trans. Antennas Propag.*, vol. 59, no. 7, pp. 2538-2545, 2011.

[17] C. Sun, S. Yang, Y. Chen, J. Guo, and Z. Nie, "An improved phase modulation technique based on four-dimensional arrays," *IEEE Antennas Wireless Propag. Lett.*, vol.16, pp. 1175-1178, 2017.

[18] A. Reyna, L. I. Balderas, and M. A. Panduro, "Time-modulated antenna arrays for circularly polarized shaped beam patterns," *IEEE Antennas Wireless Propag. Lett.*, vol.16, pp. 1537-1540, 2017.

[19] S. Yang and Z. Nie, "Mutual coupling compensation in time modulated linear antenna arrays," *IEEE Trans. Antennas Propag.*, vol. 53, no. 12, pp. 4182-4185, 2005.

[20] F. Yang et al., " Synthesis of low sidelobe 4-D heterogeneous antenna arrays including mutual coupling using iterative convex optimization," *IEEE Trans. Antennas Propag.*, vol. 68, no. 1, pp. 329-340, Jan. 2020.

[21] F. Yang, S. Yang, W. Long, Y. Chen, F. Wang, and S. Qu, "Complete and unified time- and frequency-domain study on 4-D antenna arrays including mutual coupling effect," *IEEE Trans. Antennas Propag.*, vol. 68, no. 2, pp. 824-837, Feb. 2020.

[22] J. Yang, W. T. Li, X. W. Shi, and L. Xin, "A hybrid ABC-DE algorithm and its application for time-modulated arrays pattern synthesis," *IEEE Trans. Antennas Propag.*, vol. 61, no.11, pp. 5485-5495, 2013.

[23] Y. Chen and C. F. Wang, "Synthesis of reactively controlled antenna arrays using characteristic modes and DE algorithm," *IEEE Antennas Wireless Propag. Lett.*, vol. 11, pp. 385-388, 2012.

[24] K. Guney and S. Basbug, "Null synthesis of time-modulated circular antenna arrays using an improved differential evolution algorithm," *IEEE Antennas Wireless Propag. Lett.*, vol. 12, pp. 817-820, 2013.

[25] Q. Zhu, S. Yang, L. Zheng, and Z. Nie, "Design of a low sidelobe time modulated linear array with uniform amplitude and sub-sectional optimized time steps," *IEEE Trans. Antennas Propag.*, vol. 60, no. 9, pp. 4436-4439, 2012.

[26] W. P. M. N. Keizer, "Fast low sidelobe synthesis for large planar array antennas utilizing successive fast fourier transforms of the array factor," *IEEE Trans. Antennas Propag.*, vol. 55, no. 3, pp. 715-722, 2007.

[27] W. P. M. N. Keizer, "Low sidelobe pattern synthesis using iterative Fourier techniques coded in MATLAB," *IEEE Antennas Propag. Mag.*, vol. 51, no. 2, pp. 137-150, Apr. 2009.

[28] X.-K. Wang, Y.-C. Jiao, and Y.-Y. Tan, "Synthesis of large thinned planar arrays using a modified iterative Fourier technique," *IEEE Trans. Antennas Propag.*, vol. 62, no. 4, pp. 1564-1571, Apr. 2014.

[29] Y. Chen, S. Yang, and Z. Nie, "Synthesis of satellite footprint patterns from time-modulated planar arrays with very low dynamic range ratios," *Int. J. Numer. Model,* vol.21, no. 6, pp. 493-506, 2008.

[30] Y. Chen, S. Yang, and Z. Nie, "Synthesis of optimal sum and difference patterns from time modulated hexagonal planar arrays," *Int. J. Infrared Millim. Wave*, vol. 29, no. 10, pp. 933-945, 2008.

[31] F. Yang, S. Yang, Y. Chen, S. Qu, and W. Long, "Synthesis of large-scale non-uniformly spaced 4D arrays using an IFT method," *IET Microwaves, Antennas Propag.*, vol. 12, no. 12, pp. 1973-1977, 2018.

[32] X. Huang, Y. Liu, P. You, M. Zhang, and Q. H. Liu, "fast linear array synthesis including coupling effects utilizing iterative FFT via least-square active element pattern expansion," *IEEE Antennas Wireless Propag. Lett.*, vol. 16, pp. 804-807, 2017.

[33] Y. Liu, X. Huang, K. D. Xu, Z. Song, S. Yang, and Q. H. Liu, "Pattern synthesis of unequally spaced linear arrays including mutual coupling using iterative FFT via virtual active element pattern expansion," *IEEE Trans. Antennas Propag.*, vol. 65, no. 8, pp. 3950-3958, Aug. 2017.

[34] D. M. Pozar, "The active element pattern," *IEEE Trans. Antennas Propag.,* vol. 42, no. 8, pp. 1176-1178, 1994.

[35] J. Guo, S. Yang, Y. Chen, P. Rocca, J. Hu, and A. Massa, "Efficient sideband suppression in 4-D antenna arrays through multiple time modulation frequencies," *IEEE Trans. Antennas Propag.*,vol. 65, no. 12, pp. 7063-7072, Dec. 2017.